scientific reports

Check for updates

OPEN

Target-centric analysis of hepatitis B: identifying key molecules and pathways for treatment

Xinyu Song[1,6], Jinlu Zhu[1,6], Fengzhi Sun[3,6], Nonghan Wang[1], Xiao Qiu[1], Qingjun Zhu[1]✉, Jianhong Qi[2]✉ & Xiaolong Wang[1,4,5]✉

Hepatitis B virus (HBV) poses a significant global health challenge, potentially leading to severe liver conditions, with currently limited effective treatment options available. Xiao-Chai-Hu-Tang (XCHT), a well-known Traditional Chinese Medicine (TCM) prescription, shows promise in clinical trials for treating HBV. Therefore, screening the complex components of XCHT, identifying the active compounds, and closely exploring the targets associated with hepatitis B may constitute an effective strategy for the development of new therapeutic drugs for the treatment of this disease. A systematic pharmacology and GEO chip analysis identified key targets and pathways for hepatitis B treatment and effective ingredients. Molecular docking and molecular dynamics simulation techniques were used to explore the affinity and stability of active compounds with core targets, while assessing the druggability and safety of the active compounds. The therapeutic effect of the active compound protoporphyrin in XCHT on hepatitis B were mediated through key targets such as AKT1, MAPK1, and LCK, as well as key signaling pathways like PI3K-Akt signaling pathway and Ras signaling pathway. Protoporphyrin effectively bond to active pockets of core targets and demonstrated favorable druggability and a high safety threshold. The study provided valuable insights into the development of effective treatments for hepatitis B.

Keywords Hepatitis B, Protoporphyrin, System pharmacology, Molecular docking

Hepatitis B virus (HBV) is a DNA virus belonging to the *Hepadnaviridae* group, which can cause global viral infection and mainly damages the liver[1]. The main modes of infection include mother-to-child transmission, blood-borne transmission and sexual transmission[2]. HBV infection can cause acute and chronic liver disease, such as hepatitis B. Hepatitis B is the leading cause of cancer and cirrhosis, and patients with hepatitis B have a high risk of dying from cancer and cirrhosis[3]. Despite the availability of vaccines to prevent HBV infection, the prevalence of individuals with HBV infection remains significantly high[4]. Based on data from the World Health Organization (WHO) in 2019, an estimated 296 million individuals globally are living with chronic hepatitis B, leading to 820,000 deaths annually, with 1.5 million new infections reported each year[5]. The persistence of HBV infection underscores the need for continued research into effective treatments and preventive measures, especially in light of the high mortality rates associated with its complications. It is imperative for the global health community to intensify efforts in vaccination campaigns, public health education, and the development of novel therapeutic strategies to combat this persistent threat[6]. Our study enhanced microarray analysis through data mining and conducted a secondary analysis of fundamental experiments. The study revealed a close relationship between key proteins such as RAC-alpha serine/threonine-protein kinase (AKT1), Mitogen-activated protein kinase 1 (MAPK1), and Tyrosine-protein kinase Lck (LCK) with the treatment of hepatitis B.

Holistic theory and syndrome differentiation are two major characteristics of Traditional Chinese Medicine (TCM) in the treatment of diseases[7]. TCM treatment has the characteristics of multi-ingredient, multi-target and multi-pathway, and has unique advantages in the treatment of various diseases[8]. The multi-ingredient aspect of TCM refers to the utilization of diverse sources of complex compound mixtures[9]. These components can synergistically enhance their therapeutic effects while potentially reducing side effects. The multi-target treatment approach of TCM is frequently more effective than the single-target treatment of diseases, prompting

[1]Shandong University of Traditional Chinese Medicine, Jinan 250355, China. [2]Department of Pharmaceutics, China Pharmaceutical University, Nanjing 211198, China. [3]Shandong Provincial Maternal and Child Health Care Hospital Affiliated to Qingdao University, Jinan 250014, China. [4]Key Laboratory of TCM Classical Theory, Ministry of Education, Shandong University of TCM, Jinan 250355, China. [5]Shandong Provincial Key Laboratory of TCM for Basic Research, Shandong University of TCM, Jinan 250355, China. [6]Xinyu Song, Jinlu Zhu and Fengzhi Sun contributed equally to this work. ✉email: zhuqingjuncn@hotmail.com; qjh951024@163.com; wangxl_hl@126.com

researchers to use this as a foundational principle in their studies[10,11]. Furthermore, the multi-pathway aspect of TCM underscores the ability of these treatments to modulate several biological pathways simultaneously, which can be particularly advantageous in addressing complex diseases characterized by multiple dysfunctional biological processes[11,12]. Xiao-Chai-Hu-Tang (XCHT) was recorded in *Treatise on Febrile and Miscellaneous Diseases* written by Zhang Zhongjing, a famous ancient Chinese medical scientist[13]. It is a classic Chinese medicine prescription for reconciling Shaoyang. It is composed of seven Chinese herbs: Chaihu (*Bupleurum chinense* DC.), Huangqin (*Scutellaria baicalensis* Ceorgi), Renshen (*Panax ginseng* C.A.Mey.), Banxia (*Pinellia ternate* (Thunb.) Breit.), Gancao (*Glycyrrhiza uralensis* Fisch.), Shengjiang (*Zingiber officinale* Rosc.), and Dazao (*Ziziphus jujuba* Mall.)[14]. Its efficacy is attributed not only to the individual properties of its components but also to their synergistic interactions, which together provide a comprehensive therapeutic effect. It has been reported that XCHT has the effect on anti-liver fibrosis[13–16], anti-liver cirrhosis[17], and anti-liver cancer[18]. XCHT has been used to treat liver diseases for more than 1,800 years[8]. Modern research has started to reveal the scientific foundation for these traditional applications, with studies confirming its hepatoprotective effects. This study selected XCHT as a database of traditional Chinese medicine components for the screening of active ingredients in the treatment of hepatitis B.

In this study, data mining identified 193 main active components and verified the binding activity and stability of protoporphyrin to AKT1, MAPK1, and LCK. System pharmacology, a modern pharmacological research method[19], was used for network analysis of biological systems. In summary, our study identified the potential component protoporphyrin, along with key targets and pathways relevant to the treatment of hepatitis B, utilizing data mining, molecular modeling, and microarray data analysis.

Results

Establish a comprehensive database of TCM ingredients and identify the key active components

Using oral bioavailability (OB) > 30% and drug-likeness (DL) > 0.18 as the screening criteria, 193 active ingredients in XCHT were retrieved from the TCMSP database (Table S1). Then, the network diagram of "Chinese herbs – active ingredients – targets" was constructed by Cytoscape 3.8.0 software to visualize active ingredients and protein targets of XCHT (Fig. 1) and the Degree value of active ingredients was calculated. According to the calculation, there were 369 nodes and 26,542 edges. The size of each node was set according to Degree value. The larger the node, the more connections it has with other nodes, which also suggests that the nodes play an important role in treatment hepatitis B. Concurrently, the targets of active ingredients were predicted by PharmMapper database, and all targets name were converted into gene ID by Uniport. Eventually, 445 potential targets in XCHT were obtained.

Prediction the potential targets for the treatment of hepatitis B

With "Hepatitis B" as the keyword, 1966 targets related to hepatitis B were obtained from the OMIM, GeneCards and DrugBank databases. In addition, 179 intersection targets of XCHT for treating hepatitis B were processed, the result is shown in Fig. 2.

Construction of protein–protein interaction (PPI) network

To further explore the interaction between active targets, the gene names of 179 potential targets were entered the STRING online platform, the confidence score with correlation Degree was set as "highest confidence" and the sapiens was selected as "H. sapiens", the free node were deleted, the remaining parameters keeping default, and the PPI network was obtained (Figure S1). The results indicated that the PPI network contains 151 nodes and 624 edges, the PPI network diagram was drawn by Cytoscape 3.8.0 software (Fig. 3). The top 10 targets were Proto-oncogene tyrosine-protein kinase Src (SRC), Phosphatidylinositol 3-kinase regulatory subunit alpha (PIK3R1), AKT1, MAPK1, Heat shock protein HSP 90-alpha (HSP90AA1), GTPase HRas (HRAS), Growth factor receptor-bound protein 2 (GRB2), Tyrosine-protein phosphatase non-receptor type 11 (PTPN11), LCK, and Transforming protein RhoA (RHOA).

Enrichment analysis of gene ontology (GO) function and kyoto encyclopedia of genes and genomes (KEGG) pathway

The gene names of the ingredients targets were imported into Metascape online platform for enrichment analysis, and the results were visualized by Bioinformatics online platform. The *p*-values of GO terms sorted from smallest to largest, with the top 20 items displayed in Table S2 and visualized in Fig. 4. The results indicate that the treatment process for hepatitis B may be associated with the following aspects: biological process (BP): response to hormone, protein phosphorylation, cellular response to hormone stimulus, transmembrane receptor protein tyrosine kinase signaling pathway, positive regulation of cell migration, enzyme-linked receptor protein signaling pathway, positive regulation of cell motility, positive regulation of phosphorylation, positive regulation of locomotion, response to peptide, regulation of kinase activity, positive regulation of transferase activity, positive regulation of protein phosphorylation, cellular response to nitrogen compound, cellular response to lipid, cellular response to organonitrogen compound, regulation of cell activation, response to bacterium, regulation of MAPK cascade, regulation of defense response. Cell component (CC): vesicle lumen, secretory granule lumen, cytoplasmic vesicle lumen, ficolin-1-rich granule, ficolin-1-rich granule lumen, membrane raft, membrane microdomain, side of membrane, receptor complex, extracellular matrix, external encapsulating structure, focal adhesion, external side of plasma membrane, cell-substrate junction, collagen-containing extracellular matrix, vacuolar lumen, plasma membrane raft, caveola, protein kinase complex, cytoplasmic side of membrane. Molecular function (MF): phosphotransferase activity, alcohol group as acceptor, kinase activity, protein kinase activity, kinase binding, protein tyrosine kinase activity, protein kinase binding, nuclear receptor

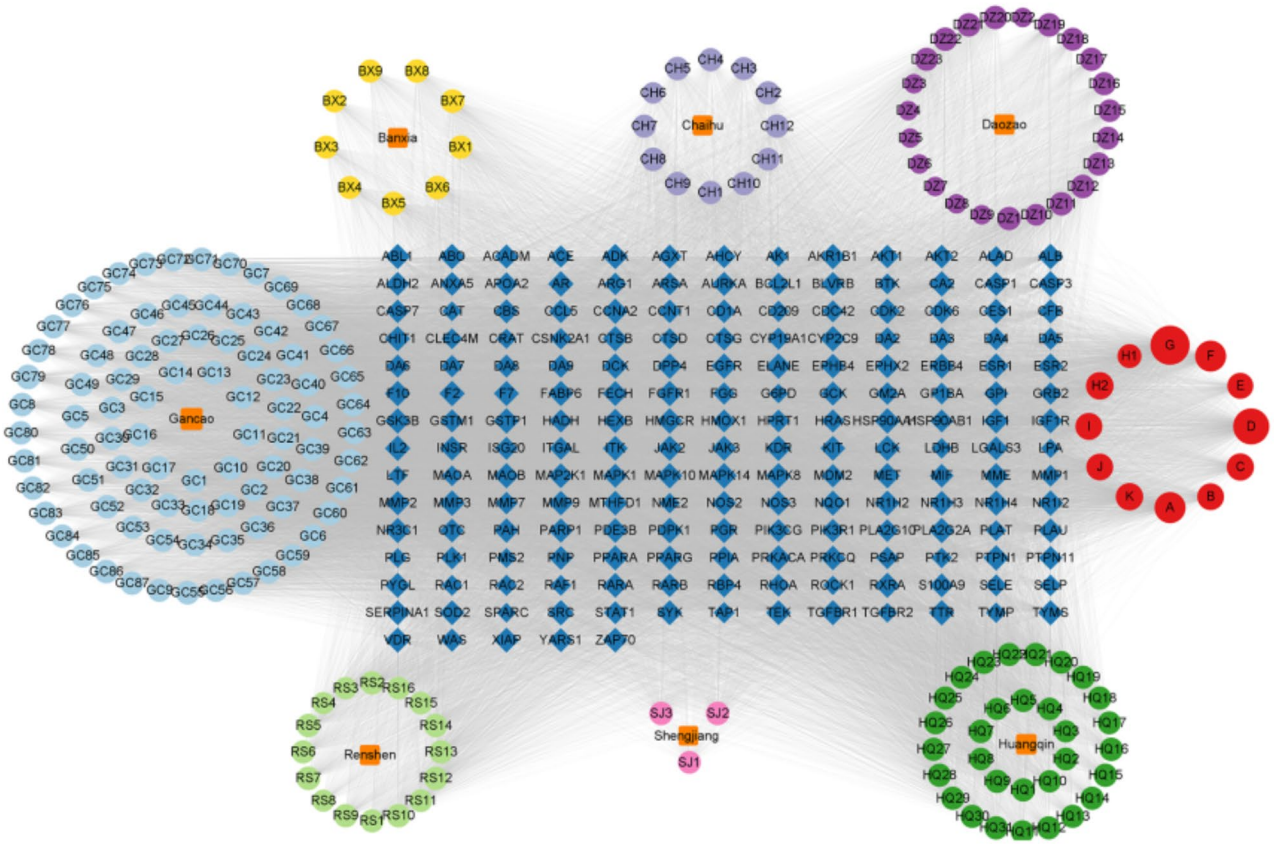

Fig. 1. The network diagram of "Chinese herbs – active ingredients – targets". The drugs and their corresponding components are organized in a circular arrangement, with the rectangular configuration serving as the targets. Blue nodes are targets, orange nodes are drugs, red nodes are the common ingredients of drugs, light blue nodes are the active ingredients of Cancao, light green nodes are nodes are the active ingredients of Renshen, pink nodes are nodes are the active ingredients of Shengjiang, green nodes are the active ingredients of Huanqin, yellow nodes are the active ingredients of Banxia, light purple nodes are the active ingredients of Chaihu, and purple nodes are the active ingredients of Dazao.

activity, ligand-activated transcription factor activity, serine-type peptidase activity, endopeptidase activity, serine hydrolase activity, kinase regulator activity, serine-type endopeptidase activity, protein serine/threonine kinase activity, protein kinase regulator activity, carboxylic acid binding, protein homodimerization activity, phosphatase binding, transmembrane receptor protein kinase activity, protein domain specific binding.

In addition, *p*-values of KEGG terms were ranked from smallest to largest, with the top 20 items displayed in Table S3 and visualized in Fig. 5. The anti-hepatitis B effect may be mediated through the following signaling pathways: Lipid and atherosclerosis (Figure S2), Proteoglycans in cancer (Figure S3), PI3K-Akt signaling pathway (Figure S4), Ras signaling pathway (Figure S5), MAPK signaling pathway (Figure S6), Chemical carcinogenesis-receptor activation (Figure S7), etc[20–22]. The results indicated that XCHT may play an important role in the treatment of hepatitis B through acting on multiple biological functions and signaling pathways.

The receiver operating characteristic (ROC) curve evaluation of the core target

The eligible GSE208535 dataset was screened in the GEO database[23], and the core target was input into the dataset for verification, and the ROC curve was drawn (Fig. 6). The area under concentration-time (AUC) score between 0.5 and 1 had predictive value, more than 0.7 indicated good diagnostic value, and more than 0.9 indicated high diagnostic value. As shown in Fig. 12, the AUC scores of SRC, PIK3R1, AKT1, MAPK1, HRAS, GRB2, LCK and RHOA were all above 0.7, and the AUC scores of AKT1, MAPK1 and LCK were more than 0.9, indicating that the diagnostic value of these targets was higher in the process of hepatitis B. Additionally, the expression of AKT1, MAPK1 and LCK in the disease group was significantly higher than that in the healthy control group, and the expression of other targets was not significantly different. Thus, AKT1, MAPK1, and LCK may serve as key targets for the treatment of hepatitis B.

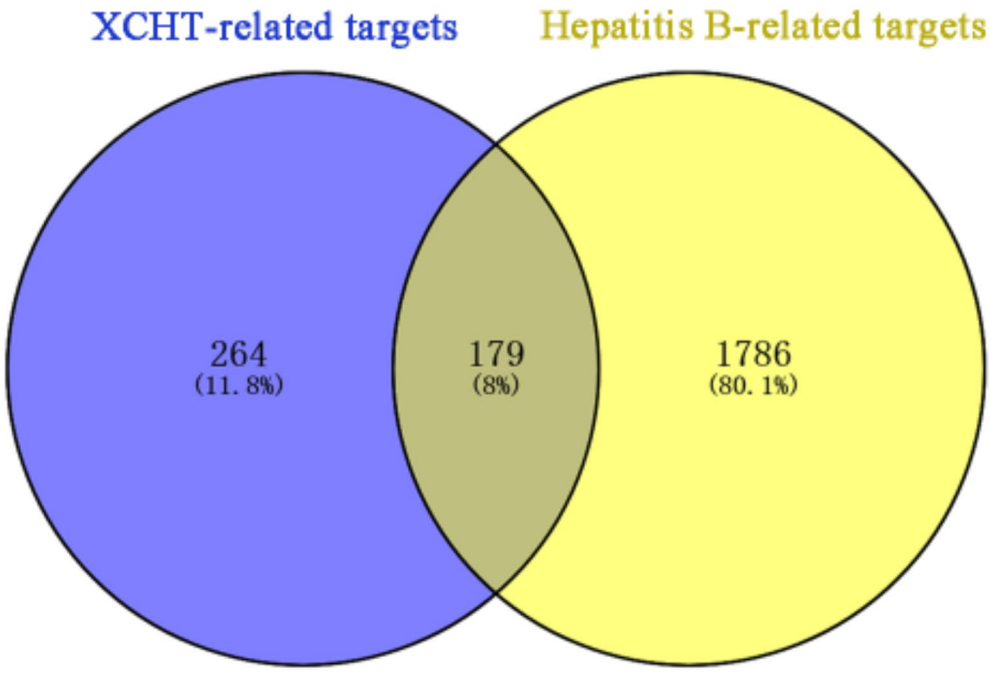

Fig. 2. Venn diagrams of XCHT-related targets and hepatitis B-related targets.

The static binding of protoporphyrin to key targets

It was reported that AKT1, MAPK1 and LCK were the key targets in the treatment of hepatitis B[24], and the binding ability of the key targets to active ingredients in XCHT was verified by molecular docking technology. The smaller of docking binding value, the more stable of ligand-receptor binding, and the greater possibility of ligand-receptor interaction. When the molecular docking fraction Affinity ≤ -4.25 kcal/mol, the binding activity between the key target and the active ingredients is considered; the molecular docking fraction Affinity ≤ -5 kcal/mol, the binding is considered to be more closer; the molecular docking fraction Affinity ≤ -7 kcal/mol, it is considered that the key target protein has strong binding activity with the active ingredients[25]. Finally, we found that protoporphyrin inhibited HBV-DNA replication[38], and had good binding ability to AKT1, MAPK1 and LCK (Table 1). Protoporphyrin exhibits superior binding affinity compared to several antiviral drugs, including Adefovir, Entecavir, Lamivudine, Telbivudine, and Tenofovir. It can be seen from Fig. 7 that protoporphyrin can be well embedded in the active pocket of the target protein, indicating that the affinity between the receptor and the ligand was strong. Also, protoporphyrin has good druggability according to the Lipinski's Five Rules (Fig. 8). Therefore, we explained the binding stability of protoporphyrin-targets complexes from the static point of view.

The dynamic binding of protoporphyrin to key targets

Considering the molecular docking results, the molecular dynamics simulation of protoporphyrin-key target composite systems was investigated, and the preprocessing procedure was shown in Figure S8-S10. Root-mean-square deviation (RMSD) revealed the position change between the later conformation and the initial conformation of proteins during MD simulation. RMSD of protein-ligand complex was an important characterization to determine whether the complex was stable. The stability of the system was tested by calculating the RMSD value within 20 ns simulation time, and the results were shown in Fig. 9a. The results indicated that backbone RMSD of protoporphyrin-key target composite systems stabilized around 0.2–0.3 nm after 8 ns, the image structure of the complex stabilizes after reaching equilibrium, and without significant conformational fluctuations. Root mean square fluctuation (RMSF) reflected the fluctuation range of each atom relative to the average position. Here, the RMSF value of amino acid skeleton atoms of the key targets were further calculated during the molecular dynamics simulation process, and the results were shown in Fig. 9b. The greater the flexibility of amino acid residues, the more significant the degree of free movement of the atoms, indicating that these regions may be

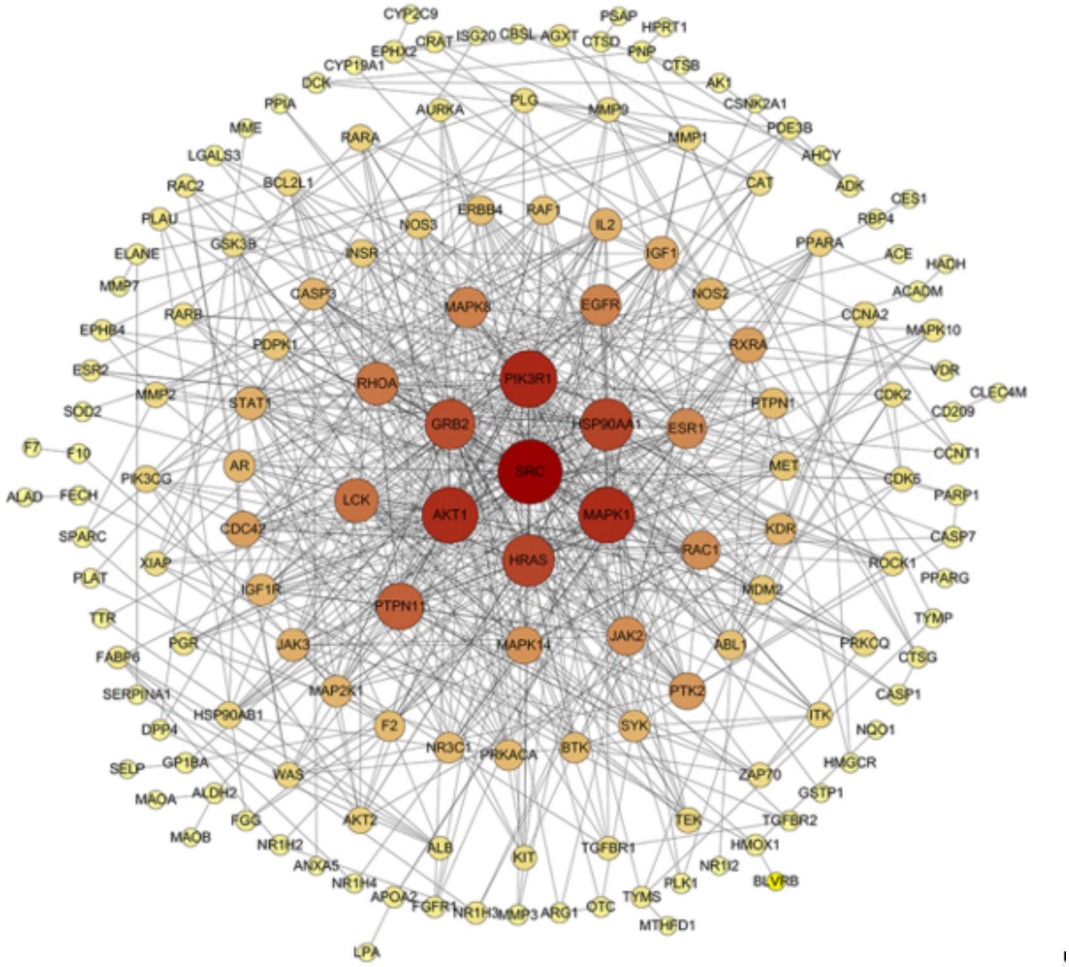

Fig. 3. PPI network of XCHT against hepatitis B. Network diagram after Cytoscape 3.8.0 processing: the size of nodes indicates the importance of targets (larger nodes denote more important targets).

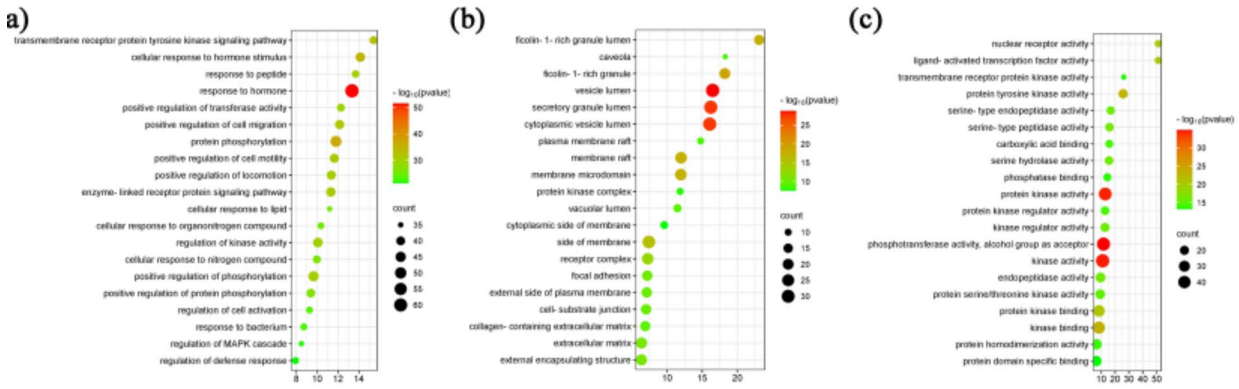

Fig. 4. Enrichment analysis of GO function. (**a**) The top 20 generatio terms in BP. (**b**) The top 20 generatio terms in CC. (**c**) The top 20 generatio terms in MF. The smaller value of *p*-value, the more important of the term.

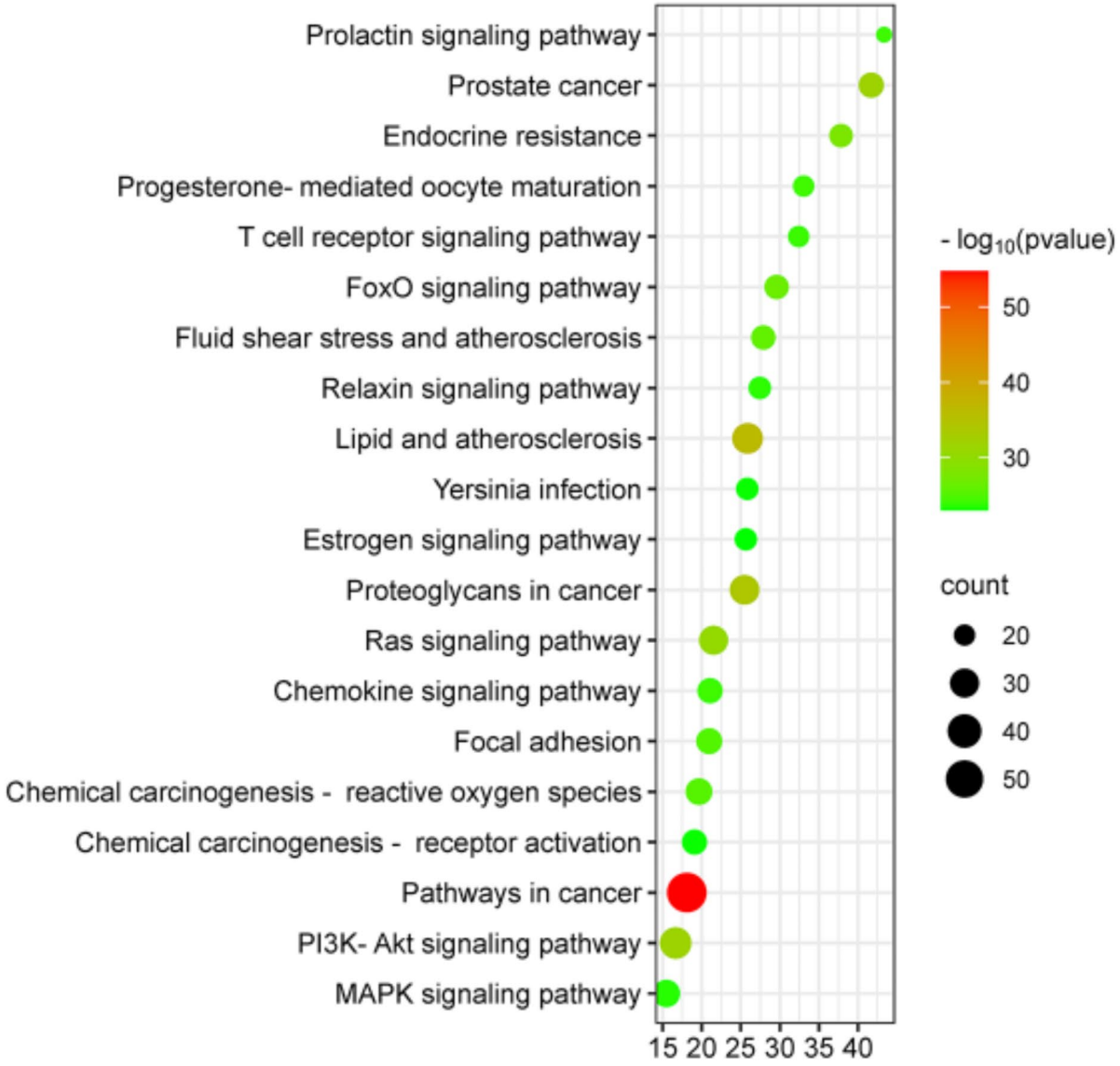

Fig. 5. The top 20 generatio terms in KEGG enrichment analysis. The smaller value of *p*-value, the more important of the term. Larger and darker areas denote more important signalling pathways.

potential active sites. The RMSF value indicated that ARG77 may be the active site for the binding of MAPK1 with protoporphyrin, LYS182 may be the active site for the binding of AKT1 with protoporphyrin, and LYS276 and LYS329 may be the active sites for the binding of LCK with protoporphyrin. The total energy change of the protoporphyrin-key target complex system was calculated, and during the simulation process, the total energy remained below -5×10^5 kJ/mol, indicating that the complex system was stable(Fig. 9c). Hydrogen bond was an important index to measure the interaction between receptors and ligands. We used geometric criteria to judge the hydrogen bonds: it was considered to be a hydrogen bond when the donor-acceptor distance was less than 3.5 Å and the donor-acceptor angle was less than 30 degrees. We analyzed the hydrogen bonds of the systems, and found that the main bonding modes of protoporphyrin-MAPK1 and protoporphyrin-AKT1 were hydrogen bonds, while the bonding modes of protoporphyrin-LCK involved other interactions (Fig. 9d). In addition, we also analyzed the binding free energy of protoporphyrin with AKT1, MAPK1, and LCK. This analysis identified the amino acids involved in the interaction and highlighted the contributions of these participating amino acids. The total energy, which resulted from the interaction of van der Waals (VDM) and electrostatic forces, indicated that a lower total energy value favored the binding of the two molecules. The results demonstrated that arginine, lysine, and histidine were involved in the binding of protoporphyrin to MAPK1 (Fig. 10a), with ARG67, ARG70,

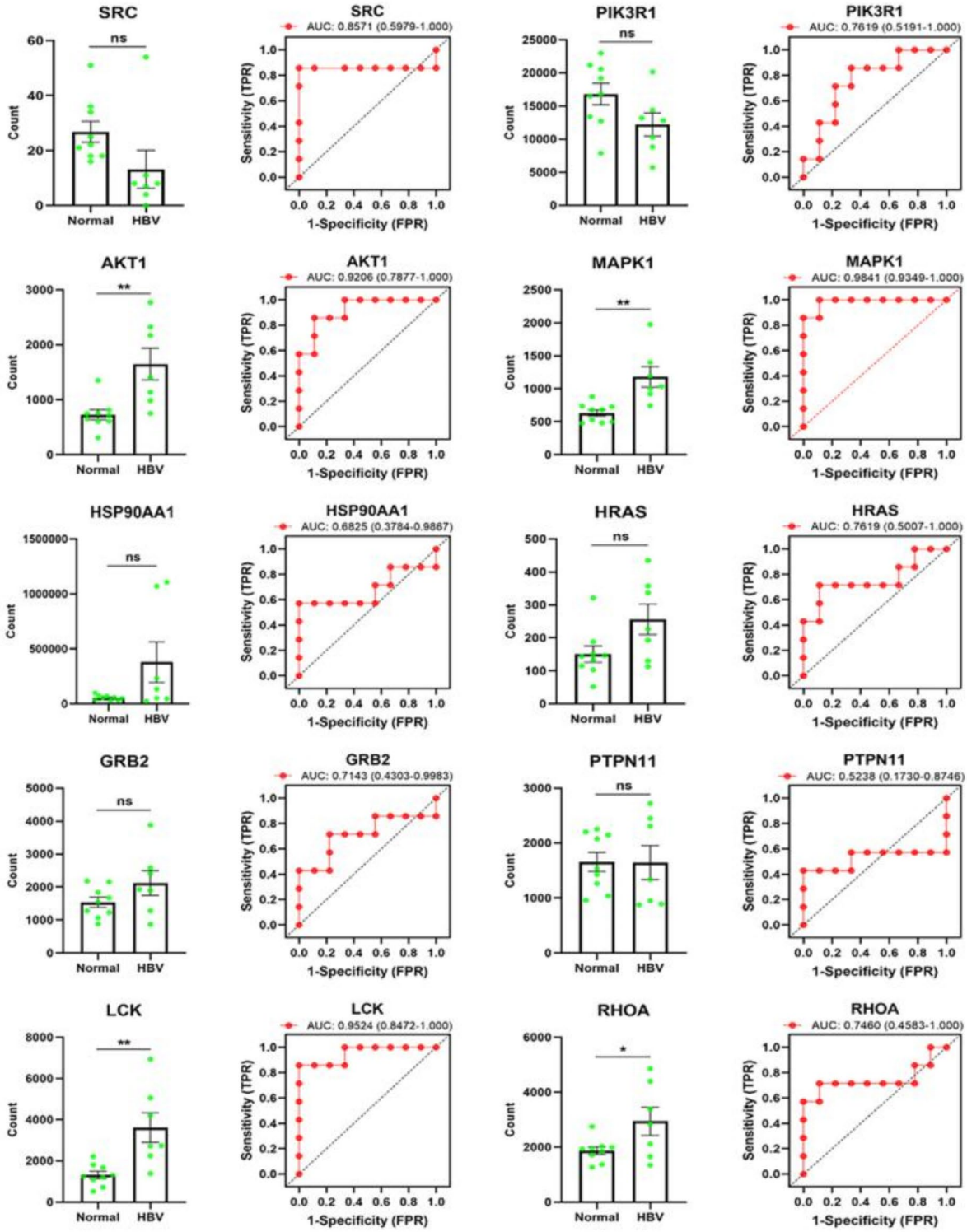

Fig. 6. ROC curve evaluation of the core target of XCHT (*$p < 0.05$, **$p < 0.01$).

ARG77, HIS147, and ARG148 contributing positively to this interaction. The binding of protoporphyrin to LCK (Fig. 10b) was associated with lysine and histidine, specifically LYS273, LYS276, LYS329, and HIS362, which enhanced the binding affinity. Similarly, the interaction between protoporphyrin and AKT1 (Fig. 10c) also involved lysine and histidine, with LYS158, LYS163, LYS182, HIS238, and LYS289 playing a significant role in facilitating this binding. Thus, the molecular dynamics simulation results confirmed that the protoporphyrin-key target complex system exhibited good stability.

Ingredient Name	Targets Name (PDB ID)	Scores (kcal/mol)
Protoporphyrin	MAPK1 (6SLG)	-9.9
	LCK (2OFU)	-9.1
	AKT1 (4GV1)	-9.0
Adefovir	MAPK1 (6SLG)	-5.8
	LCK (2OFU)	-6.4
	AKT1 (4GV1)	-6.7
Entecavir	MAPK1 (6SLG)	-7.1
	LCK (2OFU)	-6.7
	AKT1 (4GV1)	-7.5
Lamivudine	MAPK1 (6SLG)	-5.8
	LCK (2OFU)	-5.7
	AKT1 (4GV1)	-6.0
Telbivudine	MAPK1 (6SLG)	-6.4
	LCK (2OFU)	-6.6
	AKT1 (4GV1)	-6.9
Tenofovir	MAPK1 (6SLG)	-6.2
	LCK (2OFU)	-6.7
	AKT1 (4GV1)	-6.7

Table 1. The docking scores of protoporphyrin and commonly used drugs for the treatment of hepatitis B with the key targets.

The drug-likeness and toxicity of protoporphyrin

In order to further investigate the potential of protoporphyrin, we assessed its drug-likeness. The results, as depicted in Table 2, indicate that protoporphyrin adheres to the guidelines of Lipinski[26], Veber[27], Egan[28], and Muegge[29], demonstrating favorable drug-likeness. Protoporphyrin was classified as LD_{50} class-V with a value of 3066 mg/kg, indicating mild toxicity. Additionally, Protoporphyrin exhibited lower levels of Hepatotoxicity, Neurotoxicity, and Cardiotoxicity. These findings offer substantial backing for further investigations into the potential use of protoporphyrin in hepatitis B treatment.

Discussion

Currently, the Food and Drug Administration (FDA) approved drugs for children and adolescents with hepatitis B mainly including interferon-a, LAM, entecavir, peginterferon alfa-2a, and FDA approved drugs for pregnant women with hepatitis B mainly including lamivudine, telbivudine, and tenofovir disoproxil fumarate. However, most children with hepatitis B are in the immune tolerance phase, which is associated with a poor response to current antiviral therapies[30]. The currently available HBV inhibitors, including Adefovir[31], Entecavir[32], Lamivudine[33], Telbivudine[34], and Tenofovir[32], have demonstrated varying degrees of drug resistance and adverse reactions. Therefore, it is necessary to develop new drugs and methods for theI treatment of hepatitis B[35]. TCM treatment is a relatively safe and potential treatment method. It has been proved to have antiviral activity against a variety of viruses, and has fewer side effects[36]. XCHT is a classical compound of TCM to reconcile shaoyang in *Treatise on Febrile and Miscellaneous Diseases*, and it has wide range of efficacy. This study aimed to investigate the mechanisms by which XCHT treats hepatitis B, employing data mining, molecular modeling, and microarray data analysis. Based on the material basis of XCHT, the effective anti-hepatitis B active ingredients were identified through molecular docking and molecular dynamics simulation, confirming their affinity and stability with key targets.

The molecular database of XCHT was established by system pharmacology to obtain the ingredient-target, and the hepatitis B-target was obtained by DrugBank and other databases. Then, the network of XCHT in the treatment of hepatitis B was comprehensively analyzed, and the core ingredients and targets highly related to hepatitis B in XCHT were obtained. Protoporphyrin has demonstrated promising results in clinical treatment for liver cell restoration and exhibits favorable drug-likeness properties. Protoporphyrin, a significant biomolecule classified as a porphyrin compound, plays a crucial role in various key biochemical processes within organisms, particularly in hemoglobin synthesis[37]. Protoporphyrin IX (PPIX) serves as the final intermediate in the heme biosynthesis pathway, with its levels closely linked to liver diseases. The accumulation of protoporphyrin in the liver can lead to skin photosensitivity, the formation of bile pigment stones, hepatobiliary damage, and potentially liver failure[38]. Furthermore, protoporphyrin have specific applications in the treatment and diagnosis of liver diseases. For instance, sodium protoporphyrin is utilized as a liver function enhancer, promoting cellular respiration, improving protein and glucose metabolism, and exhibiting anti-complement binding properties. Additionally, the detection of protoporphyrin holds significant diagnostic value, particularly in identifying blood and liver diseases[38,39]. In summary, protoporphyrin has promising applications in the treatment and diagnosis of liver diseases, serving not only as a biomarker for liver injury but also playing a vital role in therapeutic interventions. Concurrently, its potential in drug development is noteworthy. Our study demonstrates that protoporphyrin exhibits a strong binding affinity for key targets MAPK1, AKT1, and LCK, surpassing the affinity

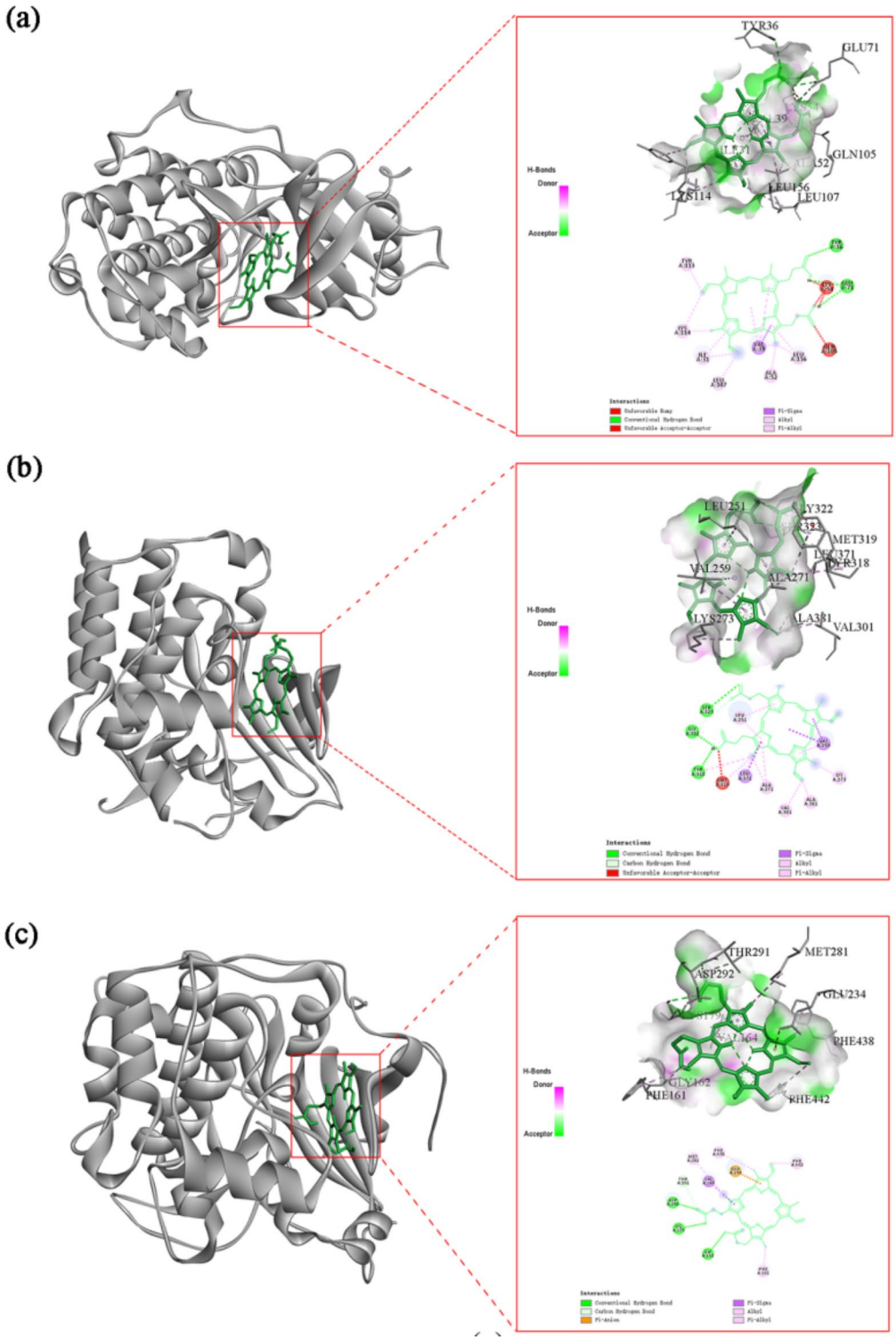

Fig. 7. The binding mode of active ingredients with targets. The 3D (left) and 2D (right) molecular models are as follows: (**a**) Protoporphyrin-MAPK1, (**b**) Protoporphyrin-LCK, (**c**) Protoporphyrin-AKT.

of commonly used HBV inhibitors for these targets. These targets are essential in the treatment of liver diseases. MAPK1 plays a role in regulating glucose and lipid metabolism essential for liver physiological functions[40], while AKT1 is closely linked to liver regeneration[41]. LCK, a member of the SRC kinase family, serves as a key regulator of various liver functions[42]. Molecular docking and molecular dynamics simulation techniques were utilized to analyze the stability and binding mode between key targets and compounds. The interaction between key

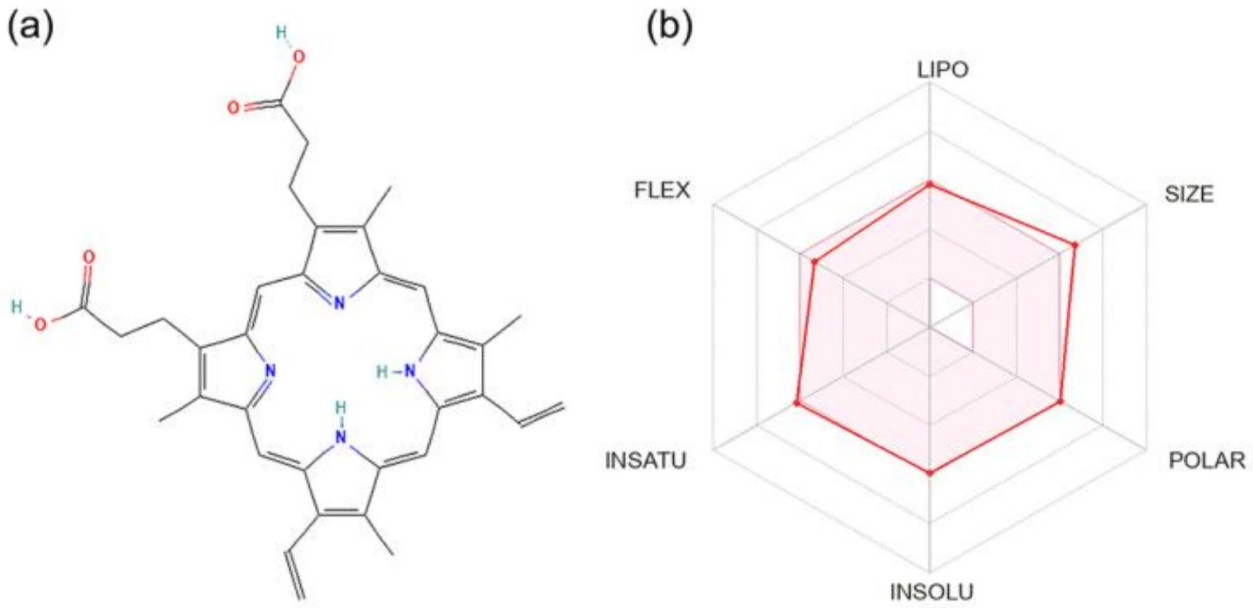

Fig. 8. Investigation of druggability of protoporphyrin. (**a**) The structure of protoporphyrin, (**b**) Druggability parameters of protoporphyrin.

targets and compounds was explained from both static and dynamic perspectives. These simulation technologies further corroborate the reliability of our data.

The GO analysis revealed that the potential targets for hepatitis B are associated with a variety of BP, CC, and MF. Notably, the BP terms highlighted the involvement of response to hormone, protein phosphorylation, and cellular response to hormone stimulus, among others. These processes are crucial for the modulation of immune responses, inflammation regulation, and metabolic pathways, which are key factors in the pathogenesis of hepatitis B[43]. The CC terms indicated a relationship between the vesicle lumen and secretory lumen granule and the key target of HBV, suggesting that this target may play a role in cell signaling and vesicular trafficking[44]. The MF terms, including phosphotransferase activity and the alcohol group as an acceptor, highlight the potential for the key target of HBV to participate in cellular signaling and metabolic pathways[45]. KEGG pathway analysis identified specific signaling pathways associated with the key targets of viral hepatitis B, including Lipid and atherosclerosis, Proteoglycans in cancer, PI3K-Akt signaling pathway, Ras signaling pathway, MAPK signaling pathway and Chemical carcinogenesis-receptor activation. The Lipid and atherosclerosis pathways are crucial for maintaining cardiovascular health, which can be compromised in individuals with chronic hepatitis B due to the systemic inflammation and oxidative stress associated with the condition[46]. The regulation of lipid metabolism and the reduction of inflammatory markers may be linked to the key targets of hepatitis B. The proteoglycans in cancer pathway highlights the significant role of proteoglycans in carcinogenesis, as they are essential components of the extracellular matrix and are associated with various cancers like liver, colon, and lung cancer. Proteoglycans in cancer are commonly used as biomarkers and therapeutic targets in hepatocellular carcinoma[47]. Furthermore, the PI3K-Akt signaling pathway is well-known for its role in promoting cell survival and growth; thus, avoiding its activation may help reduce liver damage and inhibit viral replication[48]. The Ras and MAPK signaling pathways are frequently activated in human cancer, and inhibiting their activation through the key targets of hepatitis B may prevent the progression of hepatitis B to liver cancer, thereby protecting the liver[49]. Additionally, hepatitis B is associated with chemical carcinogenesis-receptor activation, as hepatocellular carcinogenesis is causally related to chemical carcinogens that induce chronic liver injury[50]. This activation may be linked to the key target of hepatitis B by modulating various functions within these pathways and inducing liver damage through regulatory mechanisms. Moreover, this study highlights the favorable drug-likeness and low toxicity of protoporphyrin, indicating its promising potential for drug development. With its mild toxicity profile, protoporphyrin emerges as a viable candidate for treating hepatitis B. Furthermore, its strong drug-likeness guarantees the feasibility and stability during drug design and synthesis.

This study underscores the significant roles of MAPK1, AKT1, and LCK in the treatment of hepatitis B and identifies protoporphyrin with considerable potential for the development of antiviral drugs. Furthermore, it offers valuable insights into the exploration of new drug components. In conclusion, our research contributes to the advancement of safe and effective anti-HBV therapeutics.

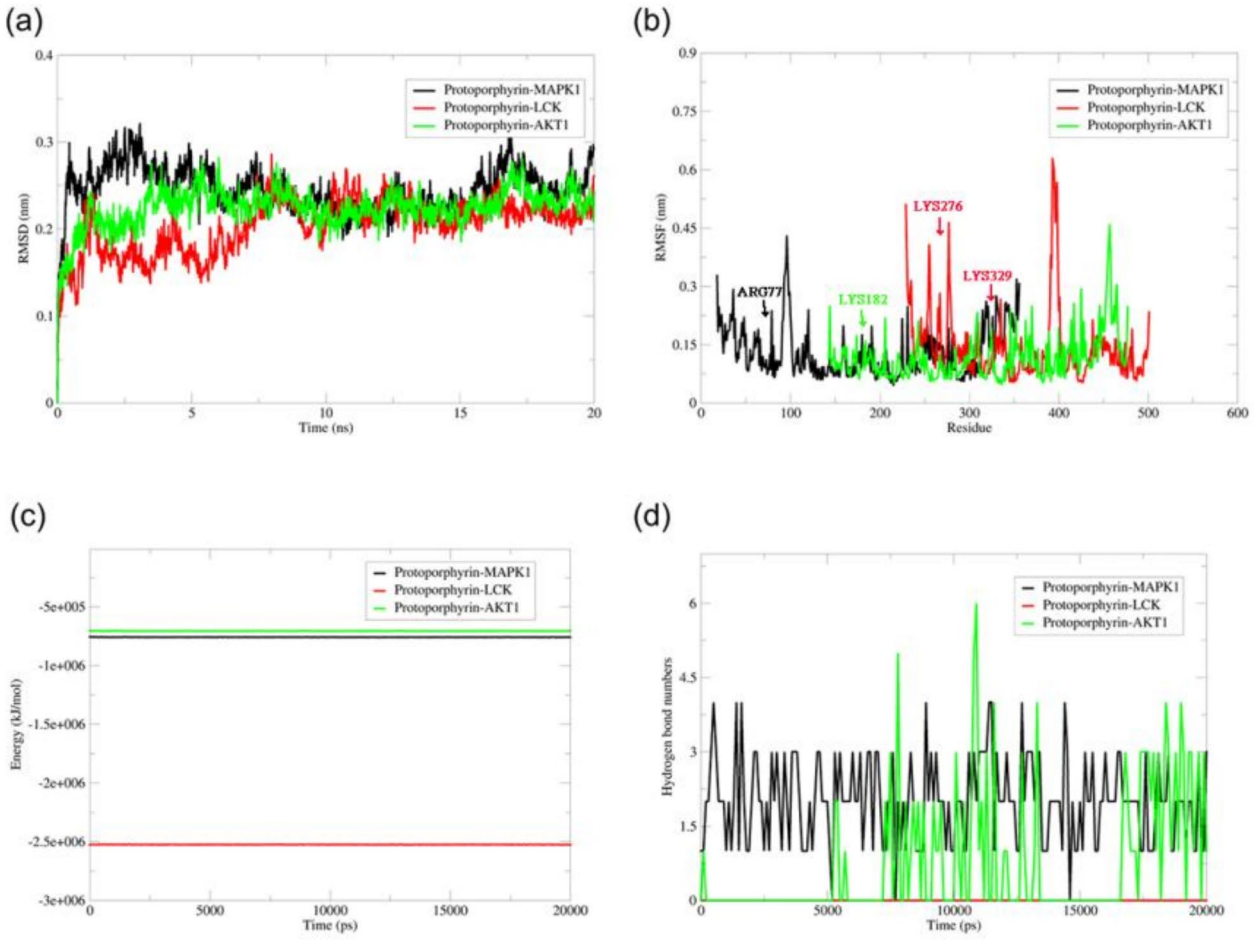

Fig. 9. Molecular dynamics simulation of protoporphyrin-key target composite systems. Black lines are protoporphyrin-MAPK1 composite systems. Red lines are protoporphyrin-LCK composite systems. Green lines are protoporphyrin-AKT1 composite systems. (**a**) RMSD, (**b**) RMSF, (**c**) Energy, (**d**) Hydrogen bond.

Methods

Establish a comprehensive database of TCM ingredients and identify the key active components

The effective ingredients of Chinese herbs in XCHT were obtained by TCMSP database (http://tcmspw.com/tcmsp.php)[51], and the core ingredients were selected by setting OB > 30%, DL > 0.18 [52]. Through PharmMapper database (http://www.lilab-ecust.cn/pharmmapper/), the targets of effective ingredients were searched. Next, the species were set as human, and the targets names were converted into gene ID by Uniprot database (https://www.uniprot.org/).

Construction of "Chinese herbs-active ingredients-targets" network

The active ingredients of Chinese herbs in XCHT were introduced into Cytoscape 3.8.0 (https://cytoscape.org/), the "Chinese herbs-active ingredients-targets network" were constructed, and the size of node protein was set according the p-value.

Prediction the potential targets for the treatment of hepatitis B

Setting "hepatitis B" as the keyword, the disease targets of HBV were obtained by OMIM database (https://www.omim.org/), GeneCards database (https://www.genecards.org/) and DrugBank database (https://go.drugbank.com/). The intersection of ingredient targets and disease targets were created by Venny 2.1.0 (https://bioinfogp.cnb.csic.es/tools/venny/), and the potential targets of XCHT in treating hepatitis B were obtained.

Establishment of PPI network

To explore the interaction of overlapping genes, the potential targets were submitted to the STRING 11.5 online platform (https://string-db.org/), and the relationship of PPI was obtained. We selected organism as "Homo sapiens", set the confidence interval to 0.9, and hid the scattered nodes[53]. To further analyze of the PPI, the

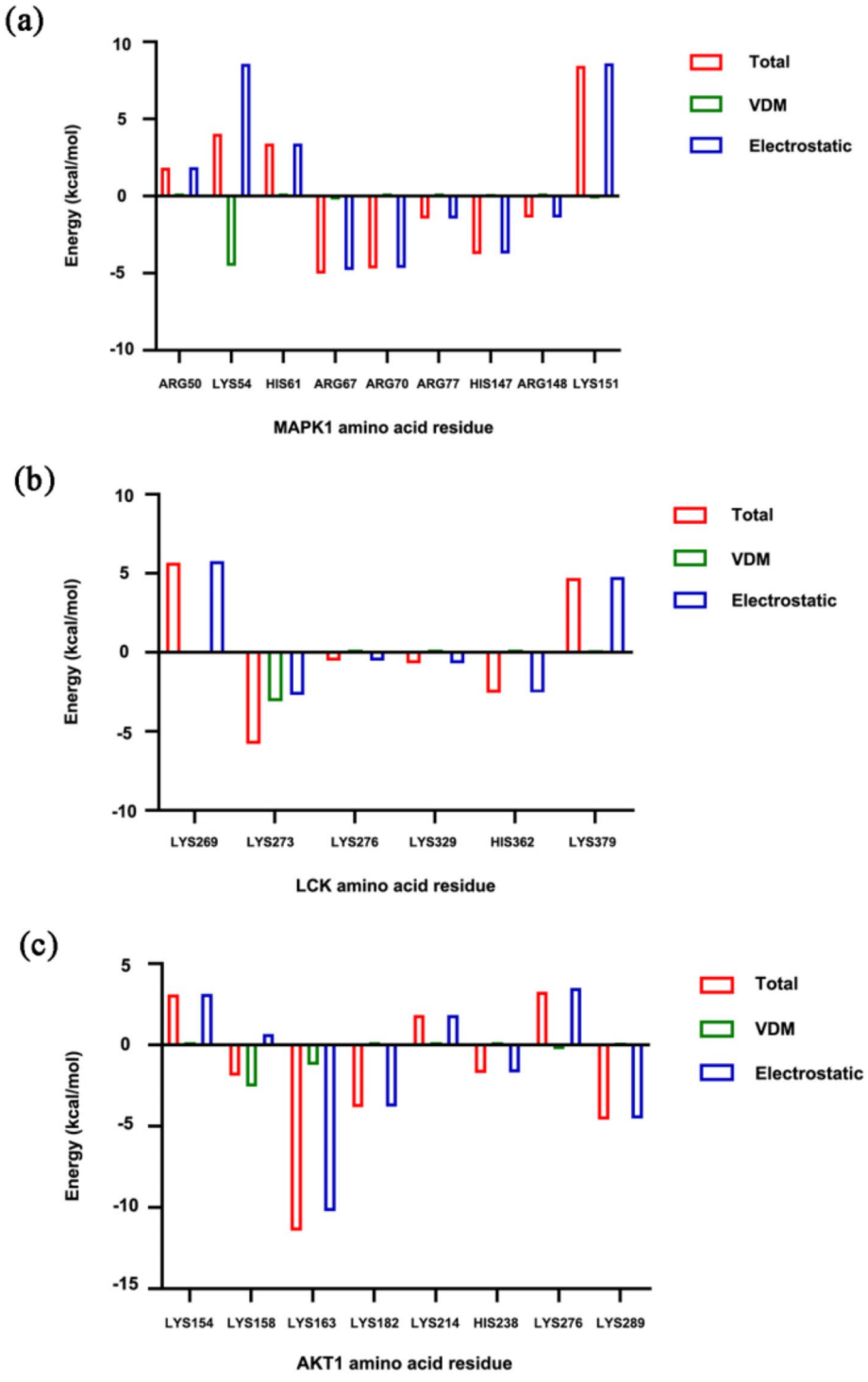

Fig. 10. Binding free energy of protoporphyrin-key target. (**a**) MAPK1, (**b**) LCK, (**c**) AKT1.

Degree and Betweenness Centrality were assessed by Network Analyze package of Cytoscape 3.8.0, and the core targets were obtained.

Enrichment analysis of GO function and KEGG

The core targets were submitted to the Metascape platform (https://metascape.org/) for GO function and KEGG pathway analysis, and the biological functions and the distribution of targets in the pathway were obtained. GO analysis included BP, MF and CC, KEGG analysis is the annotation and enrichment analysis of signaling

Name	Bioavailability Score	Drug-likeness rules					LD_{50}	Hepatotoxicity	Neurotoxicity	Cardiotoxicity
		Lipinski	Ghose	Veber	Egan	Muegge				
protoporphyrin	0.56	Yes; 1 violation: MW > 500	No; 3 violations: MW > 480, MR > 130, #atoms > 70	Yes	Yes	Yes	3066 mg/kg	Inactive	Inactive	Inactive

Table 2. The drug-likeness and toxicity of protoporphyrin.

pathways. The species was set to "H. Sapiens", mini overlap: 3, *p*-value cutoff: 0.01, mini enrichment: 1.5 [54]. The GO enrichment analysis and KEGG analysis results were visualized by Bioinformatics online platform (http://www.bioinformatics.com.cn/) according the *p*-value. Pathway diagram was modified from KEGG pathway database (https://www.kegg.jp/kegg/).

ROC curve evaluation

GEO datasets (http://www.ncbi.nlm.nih.gov/geo/) was used to find the gene chips related to hepatitis B, and Graphpad Prism v8.0.2 (https://www.graphpad.com) was used for gene expression differential analysis. The ROC curve was constructed for the core targets, and the AUC curve was used to evaluate the diagnostic value of the core targets on hepatitis B.

Molecular docking

In recent years, molecular docking methods have been widely applied to computer-aided drug research. Molecular docking is a method of drug design by simulating the interaction between receptors and ligands, which is able to predict the binding mode and affinity of targets to drug molecules[55] To further identify the effective components and targets that significantly impact hepatitis B, we employed molecular docking technology to assess the binding affinity of the active ingredients in XCHT with key targets associated with hepatitis B. Additionally, we evaluated the binding capacity of these selected key targets against commonly used drug components for HBV treatment. The drugs selected for this study include Adefovir, Entecavir, Lamivudine, Telbivudine, and Tenofovir, all of which are approved inhibitors of HBV[56]. This comparison allowed us to analyze the active ingredients we had screened. Ultimately, the compounds identified demonstrated superior binding affinity compared to the original ligands and exhibited efficacy in treating hepatitis B. Furthermore, the candidate compounds also showed enhanced binding capabilities relative to widely marketed drugs.

Firstly, the crystal structures of key targets were downloaded from the RCSB Protein Data Bank (https://www.rcsb.org/), the center coordinates of grid box were set according to the original ligand. The MOL2 structure files for the active ingredients in XCHT and the associated drug components for the treatment of HBV were downloaded from the TCMSP database using a Python script. In addition, we added polar hydrogen, assigned charge, merged non-polar hydrogen, and set rotable chemical bonds by Raccoon software, the PDBQT structure file of compound were saved. Eventually, the molecular docking of active ingredients and key targets were performed by AutoDock Vina software and python script.

Molecular dynamics simulation

Molecular dynamics simulation was conducted by GROMACS 2018.8, all simulation processes were carried out by the GROMOS96 43a1 force field[52]. During the simulation, the box was solvated with SPC water models, and the box type was set to a dodecahedron[52,57], the distance between the edge of the box and the protein edge was set to 1 nm, and the ions were added to maintain the electrical neutrality of the system. The result of molecular docking was taken as the initial structure, and the energy minimization was performed by using steepest descent minimization method[52]. Then, the system was carried out heat bath (NVT, Number of particles, Volume, and Temperature) and pressure bath (NPT, Number of particles, Pressure, and Temperature)[58]. V-rescale methods were chosen for temperature coupling, the reference temperature was set to 300 K, the step length was set to 2 fs, and the duration was set to 100 ps[59]. Parrinello–Rahman methods were chosen for pressure coupling, and the duration was set to 100 ps[59]. Finally, the molecular dynamics simulation duration was set to 20 ns and the simulation trajectories were saved. The short-range electrostatics interaction was calculated by cut-off method, and the cut-off radius was set to 1.2 nm, the Particle mesh Ewald (PME) method was used to calculate the long-range electrostatics interaction[60].

Prediction of drug-likeness and toxicity prediction

SwissADME (http://www.swissadme.ch/) was used to predict the drug-like properties of the selected ingredients[61]. The canonical SMILES notations for the selected components were obtained from the PubChem (https://pubchem.ncbi.nlm.nih.gov/) database and entered into SwissADME to calculate drug-likeness. The toxicity of the selected ingredients was tested using the ProTox 3.0 (https://tox.charite.de/protox3/), which calculated an LD_{50} value[62].

Statistical analysis

Data were presented as mean ± standard deviation (x ± s). Statistical analysis was performed using GraphPad Prism v8.0.2 software. One-way analysis of variance was used for multiple group comparisons, and t-tests were used for pairwise comparisons. $^{*}p < 0.05$, $^{**}p < 0.01$ was considered statistically significant.

Supplementary Materials: Figure S1: PPI network of XCHT against hepatitis B; Figure S2: The Lipid and atherosclerosis pathway; Figure S3: The Proteoglycans in cancer pathway; Figure S4: The PI3K-Akt signaling pathway; Figure S5: The Ras signaling pathway; Figure S6: The MAPK signaling pathway; Figure S7: The Chemical carcinogenesis-receptor activation pathway; Figure S8: The pre-processing dynamics simulation of protoporphyrin and MAPK1; Figure S9: The pre-processing dynamics simulation of protoporphyrin and LCK; Figure S10: The pre-processing dynamics simulation of protoporphyrin and AKT1; Table S1: 193 active ingredients in XCHT; Table S2: Annotation information of GO; Table S3: Annotation information of KEGG.

Data availability

The datasets used and analyzed during the current study are available from the all authors on reasonable request.

Received: 22 August 2024; Accepted: 15 October 2024
Published online: 06 November 2024

References

1. Li, J. et al. Repurposing of Antazoline Hydrochloride as an inhibitor of Hepatitis B Virus DNA secretion. *Virol. Sin.* **36**, 501–509 (2021).
2. Nguyen, M. H., Wong, G., Gane, E., Kao, J. H. & Dusheiko, G. Hepatitis B Virus: advances in prevention, diagnosis, and therapy. *Clin. Microbiol. Rev.* **33** (2020).
3. Nevola, R. et al. HBV Infection and host interactions: the role in viral persistence and oncogenesis. *Int. J. Mol. Sci.* **24** (2023).
4. Megahed, F. A. K., Zhou, X. & Sun, P. The interactions between HBV and the Innate Immunity of Hepatocytes. *Viruses* **12** (2020).
5. Wang, X. et al. Economic-related inequalities in hepatitis B virus infection among 115.8 million pregnant women in China from 2013 to 2020. *EClinicalMedicine*. **49**, 101465 (2022).
6. Kisic-Tepavcevic, D. et al. Predictors of hepatitis B vaccination status in healthcare workers in Belgrade, Serbia, December 2015. *Euro. Surveill* **22** (2017).
7. Daher, A. M., Ong, S. S. & Krisnan, D. Threat to professional autonomy and physicians' intention to use acupuncture: a study from Malaysia. *Front. Public. Health*. **10**, 820786 (2022).
8. Li, H. Advances in anti hepatic fibrotic therapy with traditional Chinese medicine herbal formula. *J. Ethnopharmacol.* **251**, 112442 (2020).
9. Xue, T. Synergy in traditional Chinese medicine. *Lancet Oncol.* **17**, e39 (2016).
10. Lo, T. Y. et al. Multi-target regulatory mechanism of Yang Xin Tang - a traditional Chinese medicine against dementia. *Chin. Med.* **18**, 101 (2023).
11. Li, L., Zhang, L. & Yang, C. C. Multi-target Strategy and Experimental studies of Traditional Chinese Medicine for Alzheimer's Disease Therapy. *Curr. Top. Med. Chem.* **16**, 537–548 (2016).
12. Ma, L. L. et al. Fever and antipyretic supported by traditional Chinese medicine: a multi-pathway regulation. *Front. Pharmacol.* **12**, 583279 (2021).
13. Hu, R. et al. Xiaochaihutang inhibits the activation of hepatic stellate cell line T6 through the Nrf2 pathway. *Front. Pharmacol.* **9**, 1516 (2018).
14. Zhang, K., Wang, Z., Pan, X., Yang, J. & Wu, C. Antidepressant-like effects of Xiaochaihutang in perimenopausal mice. *J. Ethnopharmacol.* **248**, 112318 (2020).
15. Jin, J. et al. Network pharmacology and molecular docking study on the mechanism of colorectal cancer treatment using Xiao-Chai-Hu-Tang. *PloS One*. **16**, e0252508 (2021).
16. Li, J. et al. Xiaochaihutang attenuates liver fibrosis by activation of Nrf2 pathway in rats. *Biomed. Pharmacother.* **96**, 847–853 (2017).
17. Xie, Z. et al. Favorable outcome of adjunctive traditional Chinese medicine therapy in liver cirrhosis: a large cohort study in Southwest China. *Complement. Ther. Med.* **51**, 102446 (2020).
18. Zhao, J., Liu, L., Zhang, Y., Wan, Y. & Hong, Z. The herbal mixture xiao-chai-Hu Tang (XCHT) induces apoptosis of human hepatocellular carcinoma huh7 cells in vitro and in vivo. *Afr. J. Tradit Complement. Altern. Med.* **14**, 231–241 (2017).
19. Zhang, R., Zhu, X., Bai, H. & Ning, K. Network Pharmacology Databases for Traditional Chinese Medicine: Review and Assessment. *Front. Pharmacol.* **10**, 123 (2019).
20. Ogata, H. et al. Kyoto Encyclopedia of genes and genomes. *Nucleic Acids Res.* **27**, 29–34 (1999).
21. Kanehisa, M. Toward understanding the origin and evolution of cellular organisms. *Protein Sci.* **28**, 1947–1951 (2019).
22. Kanehisa, M., Furumichi, M., Sato, Y., Kawashima, M. & Ishiguro-Watanabe, M. KEGG for taxonomy-based analysis of pathways and genomes. *Nucleic Acids Res.* **51**, D587–d592 (2023).
23. Liu, Y. et al. Increased Non-MAIT CD161 + CD8 + T cells display pathogenic potential in chronic HBV infection. *Cell. Mol. Gastroenterol. Hepatol.* **15**, 1181–1198 (2023).
24. Feng, R., Du, W., Lui, P., Zhang, J. & Liu, Y. CAPN2 acts as an indicator of hepatitis B virus to induce hepatic fibrosis. *J. Cell. Biochem.* **121**, 2428–2436 (2019).
25. Hsin, K. Y., Ghosh, S. & Kitano, H. Combining machine learning systems and multiple docking simulation packages to improve docking prediction reliability for network pharmacology. *PloS One*. **8**, e83922 (2013).
26. Lipinski, C. A. Drug-like properties and the causes of poor solubility and poor permeability. *J. Pharmacol. Toxicol. Methods* **44**, 235–249 (2000).
27. Veber, D. F. et al. Molecular properties that influence the oral bioavailability of drug candidates. *J. Med. Chem.* **45**, 2615–2623 (2002).
28. Egan, W. J., Merz, K. M. Jr. & Baldwin, J. J. Prediction of drug absorption using multivariate statistics. *J. Med. Chem.* **43**, 3867–3877 (2000).
29. Muegge, I., Heald, S. L. & Brittelli, D. Simple selection criteria for drug-like chemical matter. *J. Med. Chem.* **44**, 1841–1846 (2001).
30. Hsu, H. Y. & Chang, M. H. Hepatitis B Virus infection and the Progress toward its elimination. *J. Pediatr.* **205**, 12–20 (2019).
31. Kang, S. H. et al. Comparison of lamivudine plus adefovir therapy versus entecavir with or without adefovir therapy for adefovir-resistant chronic hepatitis B. *J. Clin. Gastroenterol.* **48**, 889–895 (2014).
32. Lee, S. et al. Tenofovir versus tenofovir plus entecavir for chronic hepatitis B with lamivudine resistance and entecavir resistance. *J. Viral Hepat.* **24**, 141–147 (2017).
33. Pallier, C. et al. Complex dynamics of hepatitis B virus resistance to adefovir. *Hepatology*. **49**, 50–59 (2009).
34. Wang, G. et al. Cost-effectiveness analysis of lamivudine, telbivudine, and entecavir in treatment of chronic hepatitis B with adefovir dipivoxil resistance. *Drug Des. Devel Ther.* **9**, 2839–2846 (2015).
35. Rahman, M. A., Ueda, K. & Honda, T. Chinese Medicine, Maoto, suppresses Hepatitis B Virus production. *Front. Cell. Infect. Microbiol.* **10**, 581345 (2020).

36. Huang, K. et al. Traditional Chinese medicine (TCM) in the treatment of COVID-19 and other viral infections: efficacies and mechanisms. *Pharmacol. Ther.* **225**, 107843 (2021).
37. Sachar, M., Anderson, K. E., Ma, X. & Protoporphyrin, I. X. The good, the bad, and the ugly. *J. Pharmacol. Exp. Ther.* **356**, 267–275 (2015).
38. Poli, A. et al. Erythropoietic protoporphyrias: updates and advances. *Trends Mol. Med.* (2024).
39. Casanova-González, M. J., Trapero-Marugán, M., Jones, E. A. & Moreno-Otero, R. Liver disease and erythropoietic protoporphyria: a concise review. *World J. Gastroenterol.* **16**, 4526–4531 (2010).
40. Saik, O. V. & Klimontov, V. V. Bioinformatic reconstruction and analysis of gene networks related to glucose variability in diabetes and its complications. *Int. J. Mol. Sci.* **21** (2020).
41. Wang, M. et al. Methyl eugenol attenuates liver ischemia reperfusion injury via activating PI3K/Akt signaling. *Int. Immunopharmacol.* **99**, 108023 (2021).
42. Zhao, H. et al. Betulinic acid prevents liver fibrosis by binding Lck and suppressing Lck in HSC activation and proliferation. *J. Ethnopharmacol.* **296**, 115459 (2022).
43. Li, H. L. et al. Identification of ellagic acid and urolithins as natural inhibitors of Aβ25–35-induced neurotoxicity and the mechanism predication using network pharmacology analysis and molecular docking. *Front. Nutr.* **9** (2022).
44. Huang, Z., Yang, Y., Fan, X. & Ma, W. Network pharmacology-based investigation and experimental validation of the mechanism of scutellarin in the treatment of acute myeloid leukemia. *Front. Pharmacol.* **13** (2022).
45. Li, S., Sun, Y. & Sun, Y. A comparative study of systems pharmacology and gene chip technology for predicting targets of a traditional Chinese medicine formula in primary liver cancer treatment. *Front. Pharmacol.* **13** (2022).
46. Mu, T., Zhao, X., Zhu, Y., Fan, H. & Tang, H. The E3 ubiquitin ligase TRIM21 promotes HBV DNA polymerase degradation. *Viruses* **12** (2020).
47. Peng, W. et al. Clinical value and potential mechanisms of COL8A1 upregulation in breast cancer: a comprehensive analysis. *Cancer Cell. Int.* **20** (2020).
48. Pósa, A. et al. Endogenous estrogen-mediated heme oxygenase regulation in experimental menopause. *Oxid. Med. Cell. Longev.* **2015**, 1–7 (2015).
49. Santarpia, L., Lippman, S. M. & El-Naggar, A. K. Targeting the MAPK-RAS-RAF signaling pathway in cancer therapy. *Expert Opin. Ther. Targets* **16**, 103–119 (2012).
50. Patel, A. et al. The unfolded protein response is associated with cancer proliferation and worse survival in hepatocellular carcinoma. *Cancers*, **13** (2021).
51. Ru, J. et al. TCMSP: a database of systems pharmacology for drug discovery from herbal medicines. *J. Cheminform*. **6**, 13 (2014).
52. Qi, J. H. et al. Feasibility analysis and mechanism exploration of Rhei Radix et Rhizome-Schisandrae Sphenantherae Fructus (RS) against COVID-19. *J. Med. Microbiol.*, **71** (2022).
53. Zhao, J. et al. Exploration of the molecular mechanism of Polygonati Rhizoma in the treatment of osteoporosis based on network pharmacology and molecular docking. *Front. Endocrinol. (Lausanne)*. **12**, 815891 (2021).
54. Liao, Y., Ding, Y., Yu, L., Xiang, C. & Yang, M. Exploring the mechanism of Alisma orientale for the treatment of pregnancy induced hypertension and potential hepato-nephrotoxicity by using network pharmacology, network toxicology, molecular docking and molecular dynamics simulation. *Front. Pharmacol.* **13**, 1027112 (2022).
55. Zhang, D., Wang, Z., Li, J. & Zhu, J. Exploring the possible molecular targeting mechanism of Saussurea involucrata in the treatment of COVID-19 based on bioinformatics and network pharmacology. *Comput. Biol. Med.* **146**, 105549 (2022).
56. Woo, H. Y. et al. Entecavir + tenofovir vs. lamivudine/telbivudine + adefovir in chronic hepatitis B patients with prior suboptimal response. *Clin. Mol. Hepatol.* **26**, 352–363 (2020).
57. Yang, P., Liu, P. & Li, J. The regulatory network of gastric cancer pathogenesis and its potential therapeutic active ingredients of traditional Chinese medicine based on bioinformatics, molecular docking, and molecular dynamics simulation. *Evid Based Complement Alternat Med: eCAM*, 5005498. (2022).
58. Liu, G., Li, Z., Li, Z., Hao, C. & Liu, Y. Molecular dynamics simulation and in vitro digestion to examine the impact of theaflavin on the digestibility and structural properties of myosin. *Int. J. Biol. Macromol.* **247**, 125836 (2023).
59. Reddy, P. S. et al. Molecular modeling, Docking, Dynamics and Simulation of Gefitinib and its derivatives with EGFR in Non-small Cell Lung Cancer. *Curr. Comput. Aided Drug Des.* **14**, 246–252 (2018).
60. Yu, R., Chen, L., Lan, R., Shen, R. & Li, P. Computational screening of antagonists against the SARS-CoV-2 (COVID-19) coronavirus by molecular docking. *Int. J. Antimicrob. Agents*. **56**, 106012 (2020).
61. Biber, G. et al. Targeting the actin nucleation promoting factor WASp provides a therapeutic approach for hematopoietic malignancies. *Nat. Commun.* **12**, 5581 (2021).
62. Karakoti, H. et al. Phytochemical profile, in vitro bioactivity evaluation, in silico molecular docking and ADMET study of essential oils of three Vitex species grown in Tarai Region of Uttarakhand. *Antioxid. (Basel)* **11** (2022).

Acknowledgements

Thanks to the Experimental Center, Medical Research Public Service Platform of Shandong University of Traditional Chinese Medicine, Shandong Provincial Collaborative Innovation Center for Antiviral TCM and Shandong University of TCM Postdoctoral Programme for their support and help.

Author contributions

Xinyu Song, Jinlu Zhu and Fengzhi Sun performed experiments, analyzed the data, and drafted the manuscript. Nonghan Wang and Xiao Qiu contributed to the data collection. Xiaolong Wang, Jianhong Qi and Qingjun Zhu were involved in the study design, data interpretation and manuscript revision. All authors contributed to the article and approved the submitted version. All authors have read and agreed to the published version of the manuscript.

Funding

This work was supported by the Shandong Provincial Natural Science Foundation of China (ZR2021LZY017).

Declarations

Competing interests

The authors declare no competing interests.

Additional information

Supplementary Information The online version contains supplementary material available at https://doi.org/10.1038/s41598-024-76567-8.

Correspondence and requests for materials should be addressed to Q.Z., J.Q. or X.W.

Reprints and permissions information is available at www.nature.com/reprints.

Publisher's note Springer Nature remains neutral with regard to jurisdictional claims in published maps and institutional affiliations.